Effect of RAP and fibers addition on asphalt mixtures with self-healing properties gained by microwave radiation heating

González-Campo, A; Norambuena-Contreras, J.; Storey, L.; Schlangen, E.

DOI
10.1016/j.conbuildmat.2017.10.070

Publication date
2018

Document Version
Final published version

Published in
Construction and Building Materials

Construction and Building Materials 159 (2018) 164–174

Contents lists available at ScienceDirect

Construction and Building Materials

journal homepage: www.elsevier.com/locate/conbuildmat

Effect of RAP and fibers addition on asphalt mixtures with self-healing properties gained by microwave radiation heating

A. González [a,*], J. Norambuena-Contreras [b], L. Storey [c], E. Schlangen [d]

[a] CIMAT, Faculty of Engineering, Universidad del Desarrollo, Santiago, Chile
[b] LabMAT, Department of Civil and Environmental Engineering, University of Bío-Bío, Concepción, Chile
[c] Department of Civil Engineering, University Federico Santa María, Valparaíso, Chile
[d] Microlab, Faculty of Civil Engineering and Geosciences, Delft University of Technology, Delft 2628 CN, The Netherlands

HIGHLIGHTS

- Microwave heating healed asphalt mixtures with RAP and metal fibers.
- The general effect of RAP was a decrease in the healing.
- The general effect of metallic fibers was an increase in the healing.
- CT-Scans showed clusters of fibers in the mixtures.

ARTICLE INFO

Article history:
Received 4 September 2017
Received in revised form 12 October 2017
Accepted 16 October 2017
Available online 4 November 2017

Keywords:
Asphalt mixture
Metallic fibers influence
Crack-healing
RAP addition
Microwave heating
X-ray microtomography

ABSTRACT

Microwave heating of asphalt mixtures containing metal fibers is a promising technology for asphalt pavement rehabilitation. The main characteristic of these types of mixtures is that they have the ability to self-heal their cracks when external microwave heating is applied. Prior to this study, the assessment of crack-healing has only been conducted in mixtures prepared with virgin aggregate materials. This paper, however, presents results of research in which the effect of adding reclaimed asphalt pavement (RAP) and metallic fibers was studied. The volumetric properties of the mixtures indicated that the air voids content increased with the fiber content. The indirect tensile stiffness modulus of the mixtures increased with the addition of RAP. Clusters of fibers were found in the mixtures by means of CT-Scan analysis. The general effect of RAP addition was a decrease in the healing of the mixtures, and the effect of fibers was an increase in the healing. Overall, it is concluded that asphalt mixtures with RAP and metal fibers have the potential for crack-healing via microwave heating.

1. Introduction

Asphalt is the most common material used for road pavement construction. For example, of the 4.3 million kilometers of roads in the United States, 94% are surfaced with asphalt [1], while in the European Union more than 90% of the road network is surfaced with asphalt [2]. Asphalt mixtures are flexible and ductile [3], have viscoelastic properties [4] that provide a good response to vehicle dynamic loads [5], their cost is normally similar to that of other pavement alternatives [3], and asphalt roads can be opened to traffic shortly after construction [6].

Despite their robust characteristics as a paving material, the quality of asphalt mixtures deteriorate with traffic and environmental factors. Cracking is one of the most common indications of asphalt pavement distress and is caused by cyclic loading (fatigue) [7], bitumen aging (oxidation) [8], and temperature variation (thermal) [9]. Cracking reduces the mechanical strength of asphalt pavements and their durability, especially when exposed to water infiltration [10]. Despite the distress associated with asphalt pavements, it is well known that asphalt mixtures have the capability of self-healing their cracks when exposed to high temperatures (e.g., during the summer season in most latitudes). This means that mixtures can close, seal, or heal the cracks independently [11] because the thermoplastic characteristic of bitumen reduces its viscosity with an increase in temperature. When asphalt pavements reach a temperature of 30–70 °C, bitumen can flow through open micro-cracks, similar to a capillary flow [12]. When pavement cools down to lower temperatures, the

* Corresponding author.
E-mail address: aagonzalez@ingenieros.udd.cl (A. González).

https://doi.org/10.1016/j.conbuildmat.2017.10.070
0950-0618/

bitumen that sealed the crack increases its viscosity, *healing* or recovering the mechanical properties of the mixture [13].

The concept of self-healing asphalt mixtures by increasing the bitumen temperature was used to create an asphalt mixture with a small content of steel wool fibers that could repair cracks [14,15]. In these mixtures, steel wool fibers absorb and conduct more thermal energy than bitumen and aggregates, increasing the electrical conductivity of the mixtures [16]. To artificially heat and heal this type of asphalt mixture, an external electromagnetic field, such as those applied by microwave devices, increases the metal fiber temperature; the heat is then transferred to the mixture, reducing the bitumen viscosity and repairing opened cracks [13–17]. Microwave radiation is a heating technique by which asphalt materials are exposed to alternating electromagnetic fields, in the order of Megahertz [18]. Previous studies have shown that microwave heating has the potential to crack-heal asphalt mixtures [19] and polymeric composite materials [20] reinforced with steel wool fibers. Nevertheless, the work conducted on the healing of asphalt mixtures by microwave heating has only considered the use of virgin aggregates and bitumen. Only recently, has metallic waste been added to asphalt mixtures to absorb and conduct heating energy in order to achieve asphalt mixtures with healing purposes using microwave heating [21]. As a result of this research, there is a high interest for increasing the use of reclaimed asphalt pavements worldwide, using different construction techniques [22,23].

Pavement recycling has technical, environmental, and social advantages over traditional construction techniques, and it is a requirement for road construction in some countries [24,25]. Therefore, it is considered important to study the healing capabilities of asphalt mixtures prepared with various reclaimed asphalt pavement (RAP) contents. The healing of asphalt mixtures with RAP could be an auspicious technique in the future, whereby small quantities of metal fibers could be added to mixtures with RAP in asphalt plants, retrofitting the mixture into one with healing capabilities by external heating. Fibers need to be added to improve the electrical and thermal conductivity of the mixtures with RAP, similarly to conventional asphalt mixtures with crack-healing properties using microwave heating.

This research aimed to evaluate the effect of adding RAP and metal fibers on the properties of asphalt mixtures with crack-healing capabilities by microwave radiation heating. With this purpose, an extensive experimental program was carried out to measure the influence of the factors mentioned above on: 1) the bulk density and air voids content, 2) the indirect tensile stiffness modulus, 3) the crack-healing properties, and 4) the volumetric distribution of fibers inside the mixtures.

2. Materials and methods

2.1. Aggregates, RAP, and bitumen

A standard dense asphalt mixture with different contents of RAP was used in the laboratory research. The RAP, aggregates, and bitumen were supplied by a local construction company in Chile. The aggregates and RAP were provided in three and two different fractions respectively (Table 1). The aggregates consisted of a 19 mm coarse gravel (Fig. 1a), a 12.5 mm gravel, and crushed dust. The RAP, in 19 mm (Fig. 1b) and 10 mm fractions, was obtained from standard pavement rehabilitation projects, where aged pavements were milled and replaced by new asphalt mixtures. The different fractions of aggregates and RAP were blended to achieve the particle size distribution of dense asphalt mixtures. The content of RAP in the mixture was 0%, 10%, 20%, and 30%, by mass. The penetration grade of the CA24 bitumen used for mixture preparation was 80/100 mm at 25 °C. A constant total bitumen of 5.2% by volume was targeted for all the asphalt mixtures. The aged bitumen content in the 19 mm and 12.5 mm RAP fractions was 3.75% and 7.06%, respectively.

2.2. Metal fibers

Steel wool fibers (Fig. 2), or simply in this paper "metal fibers" or "fibers", composed of low-carbon steel with a density of 7.180 g/cm^3 were added in small proportions to the mixtures. The metal fibers had an average diameter of 0.133 mm, with an average aspect ratio of 44 and an initial length range of 2–14 mm, which

Table 1
Particle size distribution of aggregates, RAP, and aggregates/RAP blends.

Size (mm)	Aggregates fractions			RAP fractions		Aggregate/RAP blends for different RAP contents			
	19 mm	12.5 mm	Dust	19 mm	12.5 mm	0% RAP	10% RAP	20% RAP	30% RAP
19	100	100	100	100	100	100	100	100	100
12.5	36	100	100	89	100	87	88	89	90
10	1	77	100	69	100	76	77	78	79
5	1	5	90	27	91	55	56	57	58
2.5	0	1	60	18	68	36	37	39	40
0.63	0	0	30	12	32	18	19	19	20
0.315	0	0	22	9	23	13	14	14	14
0.16	0	0	16	7	17	10	10	10	11
0.08	0	0	11	5.3	13.4	6.6	7	7.3	7.7

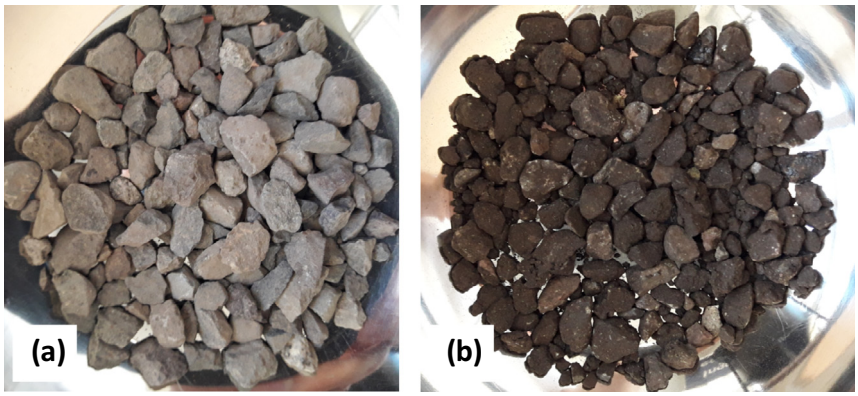

Fig. 1. The 19 mm fractions of (a) virgin aggregates and (b) RAP.

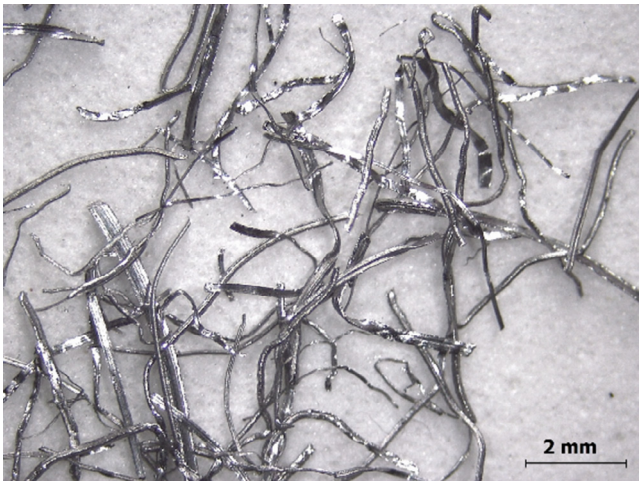

Fig. 2. Optical image of metallic fibers used in the study.

implies that both short and long metal fibers were added to the asphalt matrix. The fiber content by total volume of the bitumen were: 0%, 1%, 2%, and 4%. The mixtures without RAP were also prepared with 6% of metal fibers in order to learn the effect of a larger content of metal in mixtures with virgin materials only.

2.3. Preparation of asphalt specimens

The materials were heated for at least two hours at 150 °C before mixing. The mixing sequence for specimens with metal fibers was the following: 1) the bitumen was placed in a bowl that was previously heated in the oven to keep the mixing temperature; 2) 1% of the metal fibers was initially added to the mixture, and the remainder was gradually added after the addition of aggregate/RAP batches; 3) the blend aggregate/RAP was added in four small batches separated by particle size, starting with the batch with the largest particles. Once the particles were completely coated with fresh bitumen, the next batch with smaller particles was added to the mixture. The mixture batch was used to prepare cylindrical Marshall specimens of 100 mm in diameter and approximately 60 mm in height. For the preparation of each specimen, a sample of approximately 1200 g of mixture was compacted using a Marshall compactor, giving 75 blows to each face of the specimen. The targeted total bitumen content for each Marshall specimen was 57 g, equivalent to the 5.2% volume. Therefore, the fresh bitumen content added to the mixtures with 0, 10, 20 and 30% of RAP was 57 g, 51 g, 44 g and 37 g, respectively. The aged bitumen coming from the RAP was 0 g, 7 g, 13 g, and 20 g, for the same RAP contents. Once compacted, the specimens were cut through their diameter using a saw for asphalt to obtain two semi-circular halves. Then, each half was cut through a plane parallel to the original Marshall face to produce four semi-circular samples from one Marshall specimen. The resulting dimensions of the semi-circular samples were 100 mm in diameter and approximately 30 mm thick. In addition, a group of Marshall specimens were tested for Indirect Tensile Stiffness Modulus (ITSM) before sawing, as will be described below. Finally, a 10 mm depth notch with a thickness of 3 mm was cut at the midpoint of the semi-circular samples flat face parallel to the coaxial axis of the sample. This notch was cut to induce a crack in the three-point bending test, as described below.

2.4. Morphological characterization of metal fibers

To determine the morphological characteristics of the steel wool added to the asphalt mixtures, 120 individual fibers were selected randomly. The length and diameter of the metal fibers were determined by using an optical microscope with 35× magnification and an image software [26]. The morphological variables of metal fibers were presented in frequency histograms with the aim of comparing their length and diameter distributions.

2.5. Bulk density and air voids content

In addition to assessing the crack-healing capabilities, it was important to evaluate the bulk density and air voids content, which are physical properties of asphalt mixtures. Bulk density was calculated as the relationship between the dry mass and the real volume of each specimen, including air voids determined by water-submerged weight. The air voids content of each specimen was calculated based on the previous calculation of bulk density. Hence, as the exact percentage of materials and their density for each asphalt mixture type were known, the theoretical maximum density without voids for each specimen was found. The air voids content (AV) of each test sample was calculated as:

$$AV = \frac{\rho_{max} - \rho_b}{\rho_{max}} \quad (1)$$

where ρ_{max} is the theoretical maximum density without voids of each specimen in g/cm^3, and ρ_b is the bulk density of each specimen in g/cm^3. The bulk density and air voids content were calculated from the average of six test specimens for 17 mixture types.

2.6. Indirect tensile stiffness modulus (ITSM) tests

The stiffness of the asphalt mixtures was measured with the indirect tensile stiffness modulus test (ITSM). The stiffness was measured using European Standard UNE-EN 12697–26:2006 Annex C [27]. In the test, a vertical cyclic load is diametrically applied to the Marshall cylindrical specimen to attain a 50 εμ horizontal deformation measured using two transducers located parallel to the horizontal diameter. Ten loading pulses were vertically applied on two orthogonal diameters. The ITSM was calculated applying the following equation:

$$SM = \frac{P \cdot (0.27 + v)}{d \cdot t} \quad (2)$$

where SM is the measured stiffness modulus in MPa, P is the maximum vertical load diametrically applied in N, v is the Poisson's ratio (0.35 was adopted according to testing standards [27]), d is the horizontal maximum deformation in mm, and t is the specimen thickness in mm. ITSM tests were carried out in specimens with 2% metal fibers and RAP contents of 0%, 10%, 20% and 30%, and control specimens without RAP and without metal fibers. The tests were performed in a temperature controlled chamber at temperatures of 10, 20, 30, and 40 °C. Before testing, the specimens were left in the temperature chamber for a minimum of 4 h, to ensure that the target temperature was the same in the entire specimen volume.

2.7. Crack-healing tests by microwave radiation

The microwave healing of these asphalt mixtures was measured testing the semi-circular specimens with three-point bending tests (Fig. 3). In these tests, a vertical monotonic load was applied to the semi-circular samples until maximum load or failure. The test setup for the three-point bending tests consisted of placing the flat face of the semi-circular sample on two supporting rollers separated by 80 mm. A third loading roller was positioned at the midpoint of the semi-circular arch of the specimen (Fig. 3). A multispeed static universal testing machine, with a load cell of 50 kN and controlled by computer, was used as the loading equipment. The load speed ratio was set to 0.5 mm/min. All semi-circular samples were preconditioned at −20 °C during 24 h before the test to achieve a brittle failure. Once the bending test finished, cracked asphalt samples were left at room temperature for 3 h until they reached 20 °C, ensuring that the surface moisture resulting from freezing had completely evaporated.

Microwave heating was applied to the previously cracked semi-circular samples by using a 700 W microwave oven with a work frequency 2.45 GHz, which corresponds to an approximate wavelength of 120 mm. The heating time was set to 40 s for all samples, this time has been found suitable for microwave healing based on previous research results [18]. The room air temperature during the heating was approximately 20 °C.

The healing ratio reached for each asphalt sample, *HR*, was defined as the relationship between the maximum force of the test sample initially tested, F_0, and the maximum force measured in the test sample after the healing process, F_a, as follows:

$$HR = \frac{F_a}{F_0} \quad (3)$$

Finally, to quantify the efficiency of the repair process, a total of 7 damage-healing cycles were carried out in the test samples, completing more than 700 tests.

2.8. Temperature analysis by thermographic camera

The temperature of the semi-circular specimens was measured on their surface using a 320 × 240 pixel full color thermographic camera during 10 s immediately after heating. Temperature was measured at 43 points of the asphalt sample surface, and the data was later analyzed using a software [28]. The points were selected so that each point could represent approximately 1/43 of the measured sample face.

2.9. X-ray computed tomography (CT scan)

To analyze the distribution of the metal fibers in the asphalt mixtures with different RAP contents, X-ray micro computed tomography was conducted on samples with different contents of RAP and fiber contents. Prismatic samples with dimensions approximately 30 mm in height, 30 mm width, and 50 mm length were cut

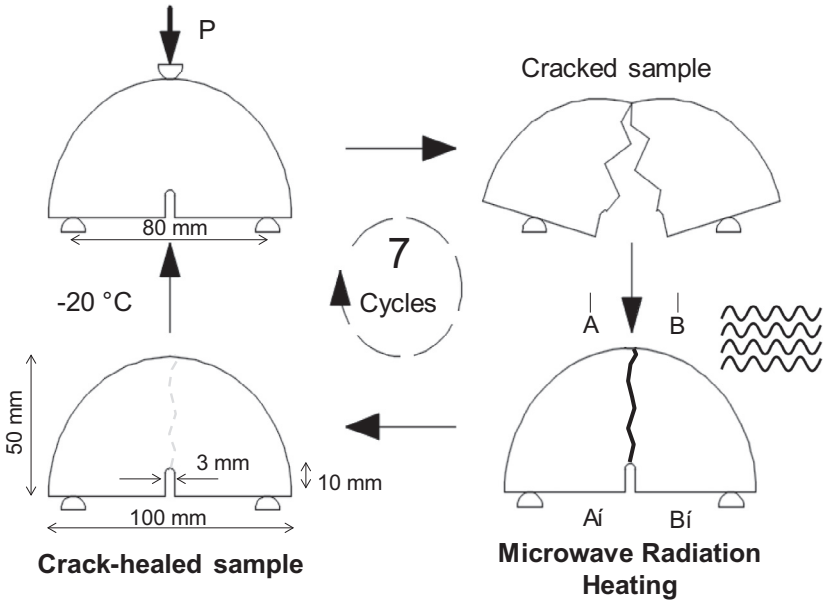

Fig. 3. Healing cycle of asphalt mixtures by microwave radiation.

from the center of the semi-circular samples after the seven healing cycles. A scheme of the vertical cuts through the semicircular specimens is shown by axes A-A' and B-B' in the bottom right of Fig. 3. The advantage of this specific cut is that it contained the healed crack and the notch, and, therefore, it was possible to identify the crack in the scan and determine whether it passed through the bitumen mastic or the aggregate.

The X-ray micro-tomography scans were obtained using a scanner operated at 160 kV and 200 μA; images were reconstructed at a spatial resolution of 25 μm (voxel side). The classification of voxels with the different types of materials in the asphalt mixture samples was achieved by segmenting voxel intensity values, which are proportional to average density of the specimen within the volume mapped by each voxel. Each sample had more than 2.4×10^9 voxels; therefore, histograms that represented the frequency or volume of each component of the mixture were able to be analyzed.

For the analysis, the first millimeters of the sample surface were discarded to avoid effects related to the sample preparation (e.g., sawing) and handling, which could result in fragments detaching from the sample. To determine an approximate spatial distribution of the metal content, for each sample a total of 12 sub-samples of approximately 2 cm^3 were taken. The bottom part of the sample that contained the notch was discarded from the analysis because, in some samples, significant deformations were observed in this area. From each sub-sample a voxel intensity histogram was generated, consisting of matrices with more than 15,000 rows. Since this was a large volume of data, scripts were programmed in a computer code [29] to handle the information. Then, a cutoff in the histogram was defined based on graphical analysis to define the voxel intensity for the fibers.

3. Results and discussion

3.1. Analysis of the morphology of metal fibers

Frequency histograms for all morphological data measured using the optical microscope are presented in Fig. 4. These histograms demonstrate that, regardless of the amount of metal fibers added to the recycled asphalt mixtures, there is an 85% probability to have long metal fibers between 4 and 8 mm, while the probability of adding shorter (<4 mm) or longer (>8 mm) metal fibers is lower (1% and 14%). As a result, the length of the metal fibers ranged from 2 to 14 mm, with an average length of approximately 5.8 mm (Fig. 4a). This value can be considered as a medium-length fiber according to published results [18]. Finally, the diameter calculated from the measurement of 120 individual metal fibers was in average 0.133 mm (Fig. 4b), which is considered a thick type of metal fiber [30]. The analysis shows that long and thick metallic fibers were added to the recycled asphalt mixtures. Since metals have good thermal conductivity, long metal fibers should increase the heating homogeneity of asphalt mixtures.

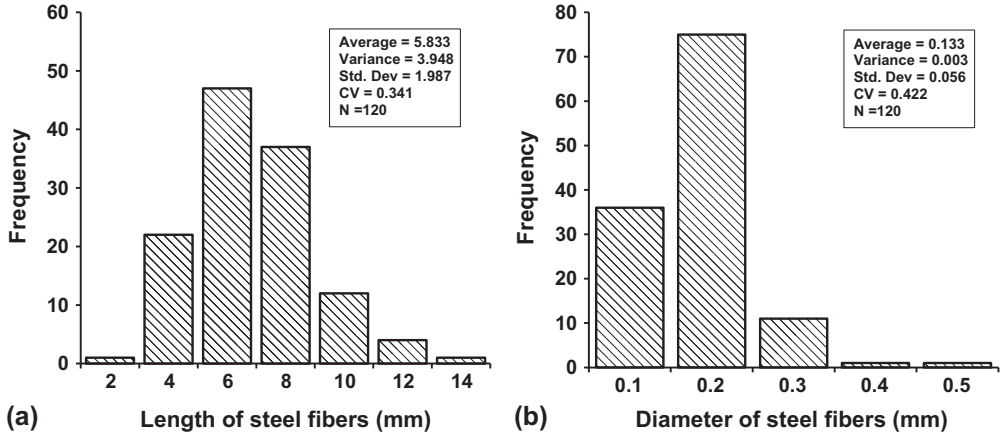

Fig. 4. Frequency histograms for the (a) length and (b) diameter of the metal fiber.

3.2. Effect of metal fibers and RAP on the bulk density and air voids content

The average bulk density for all specimens tested was 2.334 g/cm^3 (SD = 0.031 g/cm^3). No clear effect of the RAP content on the bulk density was observed, with average bulk densities of 2.331, 2.340, 2.323, and 2.339 g/cm^3 for RAP contents of 0%, 10%, 20%, and 30%, respectively. On the other hand, the average bulk density of all specimens decreased with an increase in the metal fiber content, with bulk densities of 2.353, 2.323, 2.339, 2.322, and 2.314 g/cm^3 for fiber contents of 0%, 1%, 2%, 4% and 6%, respectively. The detailed results of bulk density of asphalt mixtures are shown in Fig. 5a. As expected, the Figure shows that the mixtures with highest bulk density were those without metal fibers.

The overall average air voids content for mixtures with different fiber and RAP content was 8.0%. A general increase in the air voids content was measured with increasing fiber content. The average air voids content measured were 6.7%, 8.1%, 7.7%, 8.8%, and 10.4% for metal fiber contents of 0%, 1%, 2%, 4% and 6%, respectively. Conversely, a decrease in the air voids was measured with increasing RAP content. The average air voids content measured 9%, 7.9%, 8.0%, and 6.8% for RAP contents of 0%, 10%, 20% and 30%. Detailed results of the air voids content versus metal fibers content are shown in Fig. 5b. These results are explained because the bitumen content and aggregates remained constant in the mixtures, while the metal fiber content changed.

In addition, it was observed during the asphalt specimen preparation that mixing and compaction was more difficult for higher fiber contents. The higher air voids content is also explained by the formation of metal fiber clusters in the mixture, as shown below. The higher the metal fiber content, the higher the number of longer fibers in the mixtures, and, therefore, the probability of having clusters increases. The clusters of metal fibers make the compaction of the asphalt specimens more difficult because there is less space for the bitumen to freely flow and fill the voids within the mixtures.

3.3. Indirect tensile stiffness modulus

The indirect tensile stiffness modulus (ITSM) results for the mixtures with 2% fibers with different RAP contents are presented in Fig. 6a. In addition, ITSM for the control mixtures (0% RAP and 0% fibers) are included in that Figure. Results show that modulus decreased with increasing temperature for fiber mixtures and different RAP contents, which is explained by the visco-elastic nature of bitumen that experiences a loss of viscosity and stiffness when temperature increases, resulting in a decrease in the modulus of the asphalt mixture. Fig. 6a shows that the inclusion of 2% metal fibers reduces the stiffness of mixtures without RAP. The average stiffness considering all testing temperatures for the control mixtures without RAP and fibers was 3954 MPa, while the average stiffness considering all testing temperatures and all RAP contents for the mixtures with metal fibers was 3975 MPa. Similar stiffness were measured by Norambuena-Contreras et al. [18] in a previous research on dense asphalt mixtures. It was also observed that an increase in the RAP content increases the stiffness of the mixtures with metal fibers, which is explained by the higher stiffness of the bitumen from the RAP compared to that of the fresh bitumen. Although viscosity tests were not performed on the aged bitumen from RAP, an increase in viscosity for bitumen that has been exposed to solar radiation, high temperatures and oxygen during its service life would be expected by the volatilization of light hydrocarbon fractions, and oxidation by reacting with oxygen from the environment [31]. Regression equations were fitted to the logarithm of the measured stiffness modulus and temperatures (Table 2) with a good average R^2 of 0.988.

Fig. 6b presents the stiffness modulus measured for the test specimens in the longitudinal (A-A') and (B-B') directions, respectively. The Figure indicated that stiffness modulus in each direction (A and B) were very similar for almost all the mixtures tested, which demonstrates that the addition of metal fibers did not induce anisotropic behavior of asphalt mixtures in the plane perpendicular to the coaxial axis of the specimens.

3.4. Effect of metal fibers and RAP on the crack-healing ratios

In total, more than 700 three-point bending tests were conducted to evaluate the crack-healing of asphalt mixtures. The general effect of the RAP addition into the asphalt mixtures was a decrease in the healing ratios. For example, if the healing ratios of the seven healing cycles and all the metal fiber contents are averaged, the healing ratios of the mixtures are 0.5634, 0.4844, 0.4354, and 0.4617 for 0%, 10%, 20%, and 30% of RAP content (see Fig. 7a). Conversely, the general effect of the metal fiber content was an increase in the healing ratios. Fiber contents of 0%, 1%, 2%, 4%, and 6% yielded healing ratios of 0.4556, 0.4926, 0.4866,

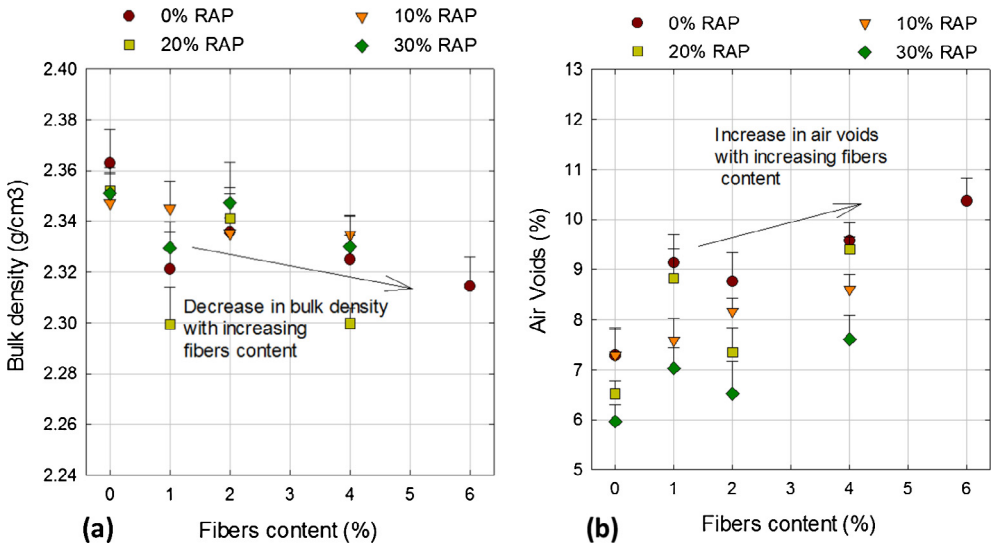

Fig. 5. Effect of metal fiber and RAP content on (a) bulk density and (b) air voids content.

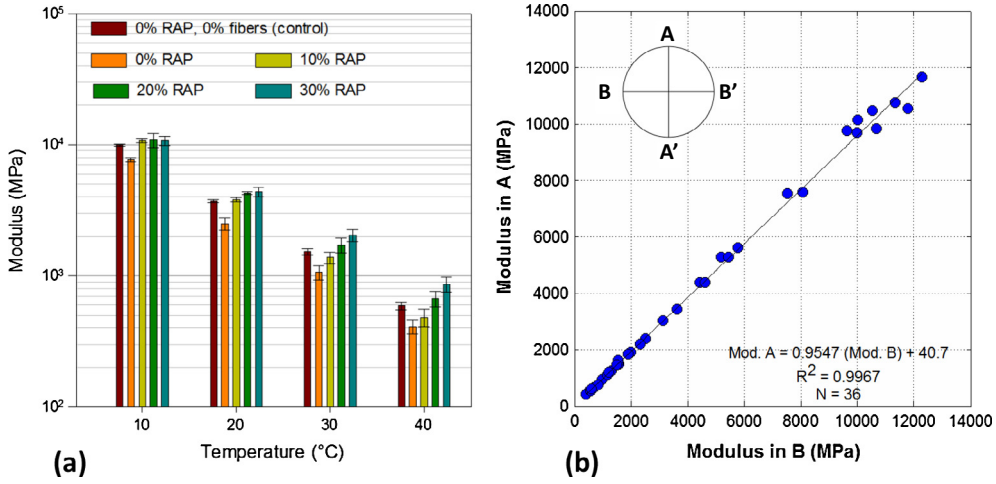

Fig. 6. (a) Indirect tensile stiffness modulus of mixtures with 2% fibers and (b) modulus measured in the longitudinal (A) and cross (B) directions.

Table 2
Linear fitting of measured stiffness modulus to temperature for asphalt mixtures with 2% steel fibers.

RAP (%)	Fibers (%)	Fitted equation ITSM in MPa, T in °C	R^2
0	0	$\log(ITSM) = 4.3997 - 0.04077 \cdot T$	0.999
0	2	$\log(ITSM) = 4.2774 - 0.04190 \cdot T$	0.990
10	2	$\log(ITSM) = 4.4796 - 0.04457 \cdot T$	0.996
20	2	$\log(ITSM) = 4.4329 - 0.04001 \cdot T$	0.991
30	2	$\log(ITSM) = 4.3804 - 0.03603 \cdot T$	0.991

0.5085, and 0.5696 (see Fig. 7b). The general effect of the number of healing cycles (see Fig. 7c) was initially an average increase of the healing ratio (from 0.4936 to 0.5409) and then a gradual decrease of the healing up to the last cycle. The initial average healing ratios were low compared to previous research studies in which microwave was used for heating the specimens. For example Garcia and Norambuena [32] found that the minimum and maximum healing ratios for the first healing cycles were approximately 0.80 and 0.96 for mixtures with 6% and 2% metal fibers, respectively. For the second cycle, they found minimum and maximum healing ratios of approximately 0.65 and 0.82 for the same metal fibers contents. Only in their fifth healing cycle were the ratios similar to the ratios for the first healing ratio obtained in this research. Sun et al. [33] found healing ratios above 0.5 for asphalt mixtures with steel fibers and steel slag healed by microwave, after nine healing cycles. In their mixtures, the average surface temperature of the specimens with fibers was similar to those used in this research, which after heating was over 98.7 °C, higher than the temperatures measured in this research, as shown below. The general effect of the RAP content in the mixtures could be explained by the higher viscosity of the aged bitumen. The mixtures with higher RAP content have a larger proportion of aged bitumen, and a lower proportion of virgin 80–100 bitumen. In other words, the 80–100 bitumen added, could be acting as rejuvenator in the new asphalt mixture, which will reactivate aged bitumen and lead to a higher binder content in the mixture. Hence, it would be expected higher healing ratios when bitumen with higher penetration grades are added to this type of mixtures.

Detailed results for the healing ratios of samples without RAP and with different contents of metal fibers are presented in Fig. 8a–d for 0%, 10%, 20%, and 30% RAP contents, respectively. In each Figure, one bar shows the average of five three-point strength tests. For the mixtures without RAP (Fig. 8a), the contribution of metal fibers to the crack-healing of mixtures was not clear, i.e., for some contents the average healing ratios increase, while for others they decrease. In addition, the average healing ratios for all the mixtures without RAP increased from the first to the third cycle, and from the fourth to the seventh cycle showed only a small decrease. Overall, the average healing ratio for the mixtures with

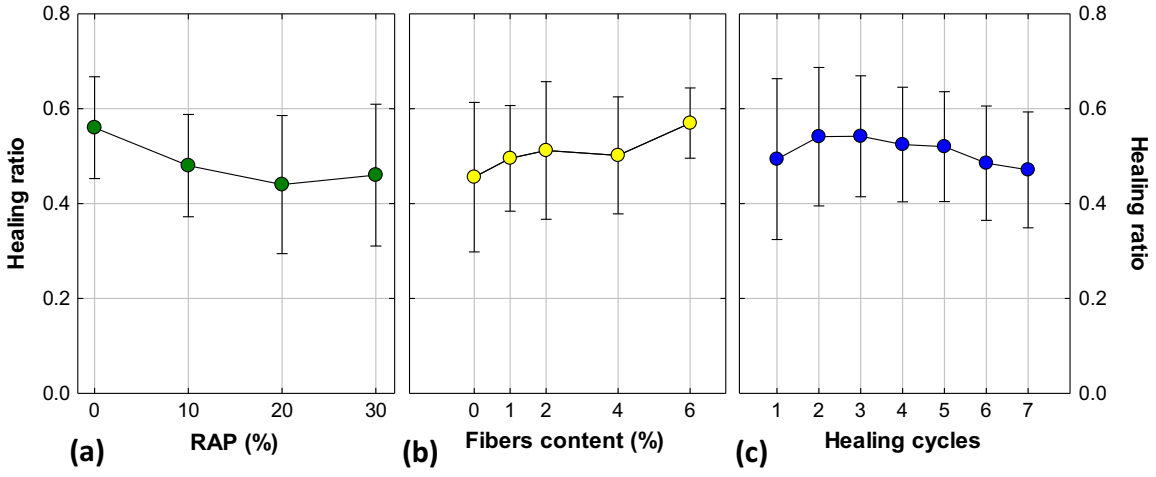

Fig. 7. General effects of (a) RAP content and (b) metal fiber content, (c) number of healing cycles.

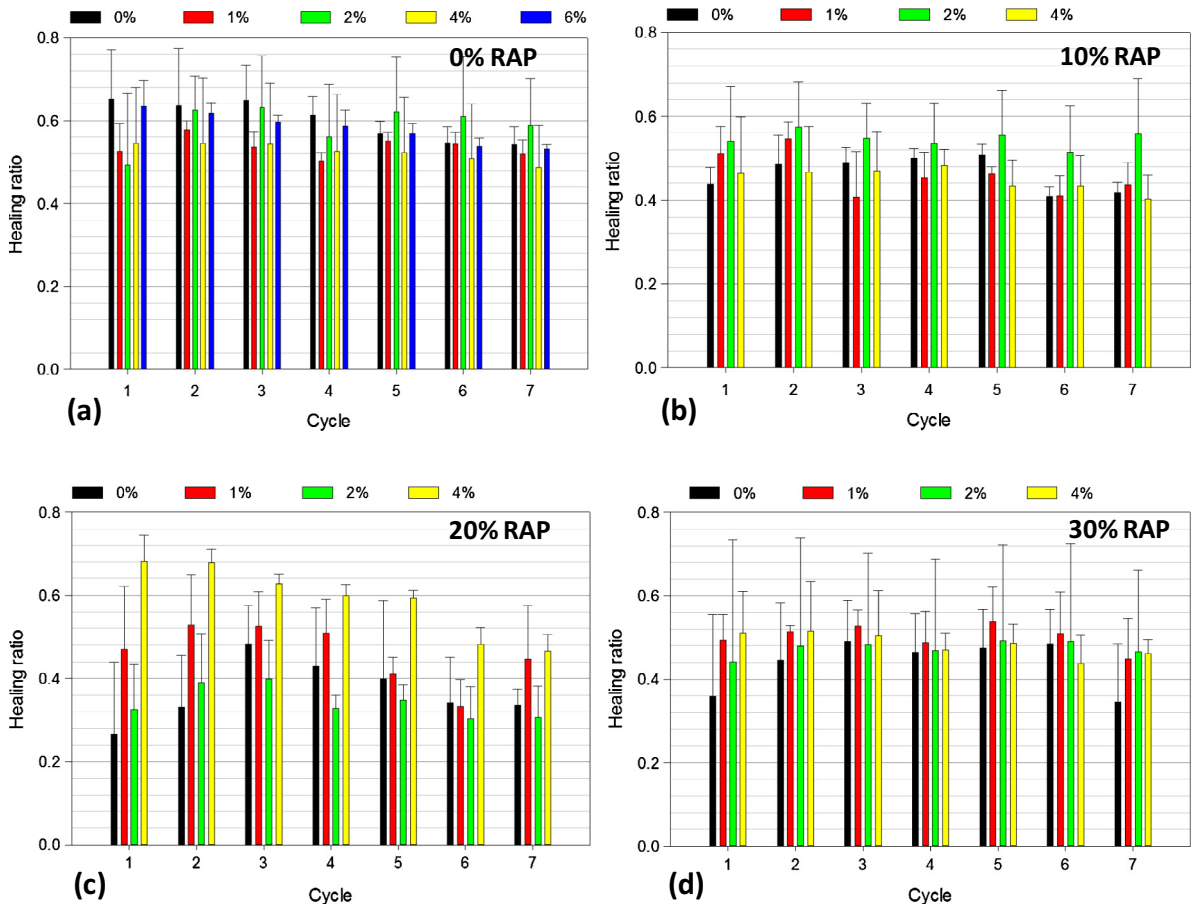

Fig. 8. Healing ratio for different contents of metal fibers and (a) 0% RAP, (b) 10% RAP, (c) 20% RAP, and (d) 30% RAP.

all the fiber contents and without RAP at the first healing cycle was 0.5505, while for the seventh cycle it was 0.5225, i.e., only a 5.5% reduction. The overall average of the healing ratio for the mixtures with 10% RAP (Fig. 8b) was 0.4844. In these mixtures, higher healing ratios were measured for mixtures with 2% fiber content. The average of the seven healing cycles was 0.4649, 0.4820, 0.5442, and 0.4464 for fiber contents of 0%, 1%, 2%, and 4%, respectively. Little difference was measured between the average healing ratios of the first healing cycle (0.4571) and the seventh healing cycle (0.4640). Nevertheless, the average healing ratios increased from the first to the second healing cycle, and then started to decrease. The only exception for the mixtures with 10% RAP was the healing ratio of mixtures with 2% fibers that remained relatively constant for all healing cycles.

The general effect of the fiber contents and number of healing cycles in the mixtures with 20% RAP (Fig. 8c) was more significant than the previous results with lower RAP contents. The average healing ratio for mixtures without metal fibers was 0.3489 (SD = 0.1506), while for the mixtures with metal fibers, the average healing ratio of the seven cycles was 0.4708 (SD = 0.1332), 0.3508, and 0.5711 (SD = 0.1002), for fiber contents of 1%, 2%, and 4%, respectively. The effect of the number of healing cycles on the healing ratios was similar to that of the previous mixtures. The healing ratio increased from the first (0.4353) to the second cycle (0.4753) and then continued to decrease until the seventh cycle (0.3749). Clearly, the mixture with 4% metal fibers showed the highest healing ratios.

The effect of the fiber content for the mixtures with 30% RAP (Fig. 8d) was an increase in the healing ratio, i.e., for metal fiber contents of 0%, 1%, 2%, and 4%, the average healing ratio for all the cycles was 0.4013, 0.4896, 0.4669, and 0.4890, respectively. The effect of the number of healing cycles was similar to the other mixtures with different contents of RAP. The healing ratio for the first cycle was 0.4395, for the second healing ratio 0.4741, and for the seventh 0.4250.

The three-point bending test with semi-circular specimens was a good method for the asphalt healing evaluation, since little damage was observed in the specimens after the seven healing cycles. Damage was reported by Norambuena-Contreras and Garcia [32], who observed that microwave heating can overheat and damage specific areas of the semi-circular asphalt specimens. Nevertheless, the average healing ratios remained relatively constant, showing that specimens could be reused for the seven cycles.

3.5. Temperature analysis of samples

The temperature analysis was performed using a specialized software [28]. For each specimen, the temperature was recorded for 10–12 s immediately after the 40 s microwave heating was finished. Then the microwave door was opened with the infrared camera recording. To obtain representative results, temperature was obtained in 43 points of the sample surface. The location of each point was selected so that each point covered approximately the same area of the specimen face (91.3 mm^2 total area). Since the time was recorded for 11 s, a total of $43 \times 11 = 474$ points were recorded in each test. Outliers were detected in the data collection; hence, the 10 maximum and minimum 10 temperatures collected were eliminated from the analysis, with a total of 454 data for each temperature measurement. Typical infrared images obtained at t = 10 s for a sample without RAP and 2% metal fibers, and for a sample

with 30% RAP and 4% metal fibers are shown in Fig. 9a and b, respectively.

The average temperatures during the 11 s tests ranged from 54 to 87 °C, with a general average of 69 °C. The detailed temperature results for each sample are shown in Fig. 10. The average of temperatures measured in samples without RAP was 67.0 °C (SD = 9.3 °C); whereas, 75.3 °C (SD = 7.9 °C), 71.4 °C (SD = 7.2 °C), and 67.4 °C (SD = 3.3 °C) were measured as averages for specimens with 10%, 20% and 30% of RAP, respectively. The average temperature for specimens with fiber contents of 0%, 1%, 2%, and 4% were 70.2 °C (SD = 7.5 °C), 70.6 °C (SD = 12.9 °C), 67.8 °C (SD = 4.0 °C), and 67.3 °C (SD = 3.99 °C), respectively. Therefore, no clear effect could be established between measured surface temperature and RAP content. Similarly, no overall effect could be established between metal fiber content and surface temperature. The temperatures obtained are lower compared to those of other studies [33] where the average temperature after heating was 98.7 °C, and the healing ratios were higher than those obtained in the present study. Conversely, in a separate study [32], surface temperatures of 45–60 °C were obtained, and healing ratios were higher than those obtained in this research.

Results also show that samples without fibers could be heated between 60 and 80 °C because microwave is optimized to heat compounds with polar molecules such as bitumen [32], and also because aggregates contained metals that can be heated with microwave radiation [34,35]. Metals were detected in CT-Scan results, detailed below in this paper. To verify that aggregates could be heated without metal fibers, approximately 500 g of the 19 mm aggregate fraction of the mixture (Fig. 1a) was microwaved for 60 s. As a result, the temperature of the aggregate measured with an infrared thermometer increased to 106.3 °C immediately after heating, showing that aggregates could absorb heat.

3.6. Evaluation of the CT-Scan results

3.6.1. Analysis of voxels histograms

In the histogram of the voxel values, the transition between air and solids was a null in the derivative of the histogram values. Nevertheless, transition from bitumen to aggregate was less apparent, and was identified as the first maximum in the derivative of the histogram at voxel values above the air-solids transition. Due to the relatively low spatial resolution of the reconstruction of the CT-Scan images, as compared to the diameter of the metal fibers, it was not possible to clearly identify a definitive marker for the transition between aggregate and metal fibers. Nevertheless, the image filter options of the reconstruction software helped to identify an approximate threshold between aggregates and fibers by visual inspection. Metal particles were also observed in the aggregates, which were difficult to separate from the metal fiber count because the aggregates had similar densities to the fibers. Finally, a threshold was defined for the transition from aggregates to fibers for all the CT-Scan analyses conducted, and results were consistent with the metal fiber contents added to each asphalt mixture.

3.6.2. Spatial distribution of fibers in the mixture

For the analysis of the spatial distribution of metal fibers, each sample scan was virtually subdivided into 12 volumes of approximately 1.8 cm^3, using a software for CT-Scan analysis [36] (Fig. 11). For each sub-sample, the histograms containing the frequency of

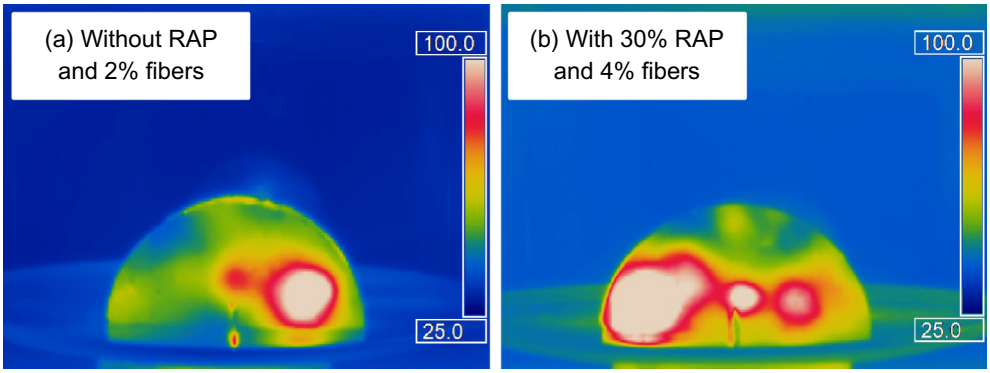

Fig. 9. Infrared temperature profiles for asphalt samples heated by using microwave radiation.

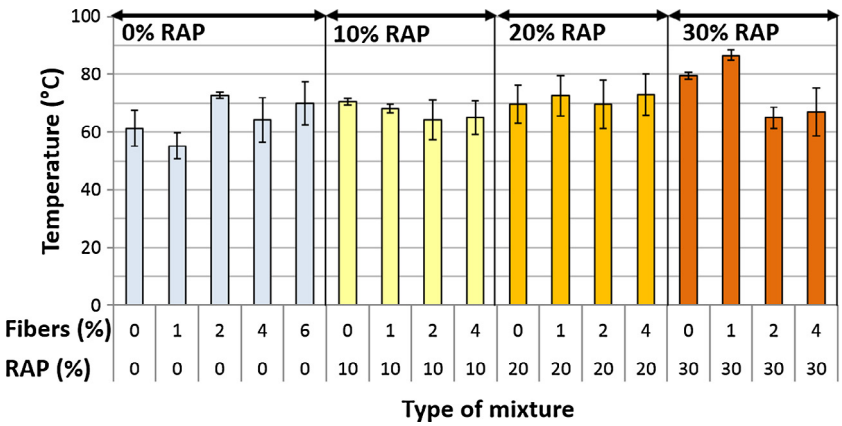

Fig. 10. Average of surface temperatures measured after heating, in samples heated in microwave.

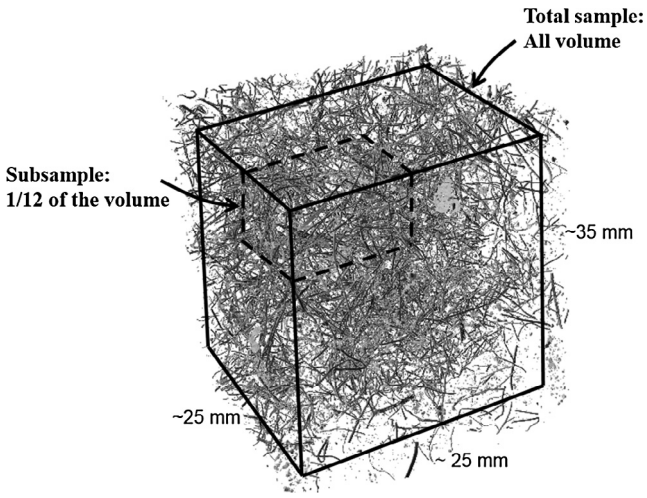

Fig. 11. Partition of the volume analyzed in the CT-Scans.

voxels were exported to spreadsheets for detailed analysis using scripts written in a computer code [29]. In addition to the calculation of the fiber contents for the 12 sub-samples, the fiber content for the total sample was calculated. Little difference between the fiber content in the total sample, and the 12 sub-samples should be obtained in mixtures with a homogeneous metal fiber distribution. Conversely, a mixture with poor fiber distribution should concentrate the metal fibers in specific spots of the sample, and therefore it would be expected to find a large difference between the fiber content in the total sample some of the 12 sub-samples. Since it was difficult to match exactly the fiber content of the mixtures analyzed with the CT-Scan results, correction factors to approximately equal the fiber content with the measured content were introduced into the analysis to achieve a better agreement between the CT-Scans and the known material proportions of the mixtures. The adjustments applied, however, do not affect the objective of calculating the spatial distribution of metal fibers, since the fiber content calculation for all the sub-samples and total sample was equally affected by the analysis.

The results for the spatial analysis are shown in Fig. 12. The bars represent the calculated fiber content for each sub-sample, and many sub-samples had a metal content similar to the target contents of the mixtures; however, for some sub-samples the metal content doubles the target value. For example, sub-sample 10 for the mixture with 30% RAP and an average fiber content of 2% shows a fiber content of 4.9%. Similar results were observed for samples with 0% RAP and 2% fibers (see sub-sample 11) and sub-samples 6 and 10 for mixture with 30% RAP and 2% fibers. This analysis shows that spontaneous fibers concentration occurs in mixtures with and without RAP, and for different fiber contents, despite the efforts made during the mixing phase in the laboratory to avoid clustering of fibers. In addition to the fiber clusters, metal concentration was observed in some aggregates. For example, in the mixture with 0% RAP and 4% fibers, 7.9% of metal in sub-sample 1 is explained by an aggregate with higher metal concentration.

To confirm the numerical analysis of the histograms, three-dimensional and cross-sections images of the CT-Scan were thoroughly analyzed. The three-dimensional image for the mixture with 2% fibers and 30% RAP is shown in Fig. 13a. In the Figure, it is possible to see a cluster of metal fibers that belongs to the sub-sample with the highest concentration of fibers mentioned above. The three-dimensional image for the mixture with 4% fibers and 0% RAP is shown in Fig. 13b, where the metal concentration from aggregates is shown in the upper left part of the sample. Note that metal from the aggregates is shown as small dots or spheres instead of the long thread shape of the fibers. In addition, it is clear that the overall higher concentration of fibers of Fig. 13b compared to Fig. 13a, explains the higher air voids in mixtures with higher fibers contents. The denser concentration of fibers, makes it more difficult for the bitumen mastic to flow and fill the voids.

3.6.3. Qualitative analysis of aggregate fracture and fibers through the cracks

A qualitative analysis of the cracks produced by the three point tests, and the fiber location through the cracks was performed examining the CT-Scan images. For a faster analysis, the images were organized in sequences using an image software [26], so that it was possible to identify the cracks and fibers by superposing several images of the sample cross sections. The analysis showed that the cracks induced by the three point tests started from the notch and then typically followed the mastic of the asphalt mixture or the transition between the mastic and the larger aggregate particles. In addition, cracking of the aggregates was observed in the CT-Scan top view images of the specimens tested (see Fig. 14a). The very stiff condition of the bitumen at the testing temperature of −20 °C favored the crack propagation through the aggregate. The fracture of the aggregates does not favor the healing of asphalt mixtures, since the fractured surface does not contain bitumen that can flow and seal the crack when heated under microwave radiation. Nevertheless, after several healing cycles the bitumen could flow to the aggregate fractured surface and improve the crack-sealing. Although this phenomenon was not investigated in this paper, it should be further analyzed in future research.

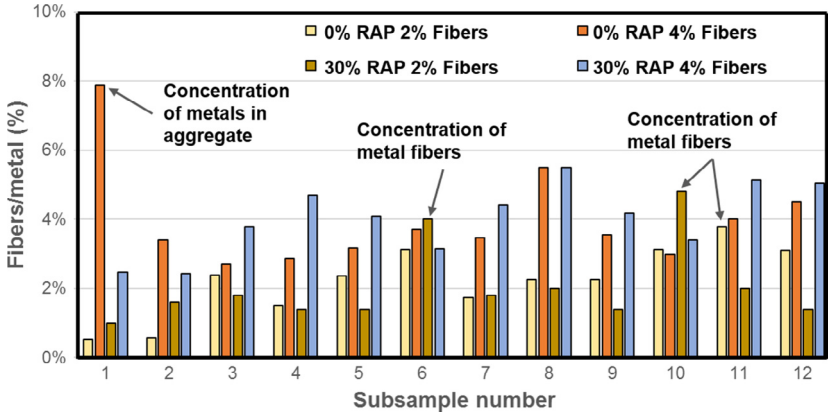

Fig. 12. Metal fiber content for each sub-sample.

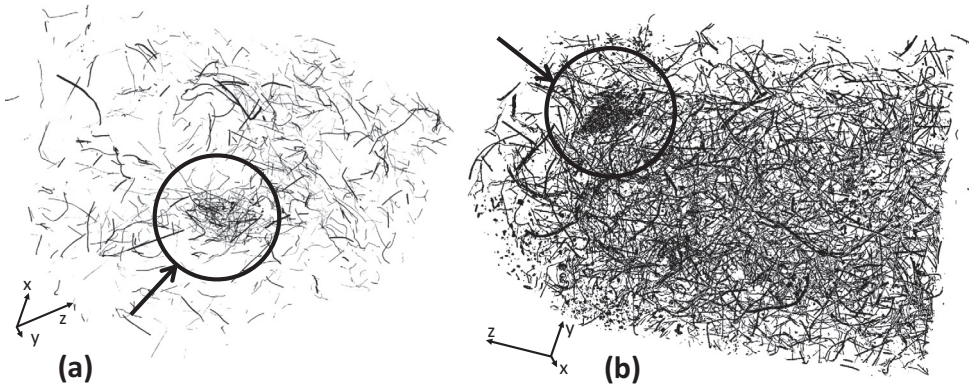

Fig. 13. Three-dimensional reconstruction of samples with (a) 2% fibers and 30% RAP and (b) 4% fibers and 0% RAP.

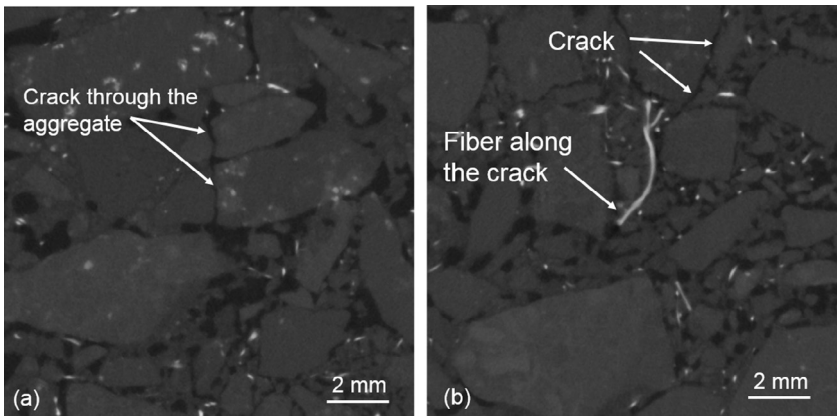

Fig. 14. Top cross-section of the samples after seven healing cycles (a) cracking through the aggregate and (b) fiber orientation throughout the crack.

In addition to the aggregates, the condition of the fibers through the crack was examined with the CT-Scan images (see Fig. 14b). Fracture of fibers was not observed, indicating that the strength of the fibers can withstand three point strength test loads. Nevertheless, it was apparent that, during the heating, fibers align with the direction of the crack, following the fracture trajectory, which could be caused by the bitumen flow and when, after fracture in three point tests, the two parts of the samples are held together, pushing the fiber onto the fractured face. The orientation of the fibers in the direction of the crack should improve the healing since the healing will cover a larger surface of the fractured face, helping the bitumen to flow throughout the crack.

4. Conclusions

This paper has explained the effect of adding RAP and metal fibers on the properties of asphalt mixtures with crack-healing capabilities gained by microwave radiation heating. Based on the analysis of results, the following conclusions can be drawn from this study:

- No clear effect of the RAP content was observed on the bulk density of the mixtures, while a decrease in the bulk density was observed for increasing fiber content. Conversely, a decrease in the air voids was measured with increasing RAP content, and a general increase in the air voids content was measured with increasing fiber contents.
- The indirect tensile stiffness modulus of mixtures with a constant fiber content increased for increasing RAP contents, while the stiffness modulus decreased with increasing temperature for fiber mixtures and different RAP contents. The addition of fibers does not induce anisotropic behavior of asphalt mixtures with RAP in the plane perpendicular to the coaxial axis of the specimens.
- The general effect of the addition of RAP into the asphalt mixtures was a decrease in the healing ratio. Conversely, the general effect of the fiber content was an increase in the healing of the mixtures.
- The average surface temperature of the asphalt samples after microwave heating ranged from 54 to 87 °C, with an average of 69 °C.
- Clusters of fibers were found from CT-Scan images although during the mixing particular care was taken to reduce this effect. It was found that the aggregate particles of the mixtures contained metals, which explains the heating of samples without fibers. Also, it was found from CT-scans that aggregates not coated by bitumen were cracked during the three point bending tests, leaving parts of the cracked surface not coated with bitumen.
- Overall, it is concluded that asphalt mixtures with up to 30% of RAP and metal fibers have the potential of being crack-healed by microwave heating.

Acknowledgments

The authors would like to thank: José Luis Concha from LabMAT at the UBB, Elber Gajardo and Horacio Moya from CIMAT UDD, Shi Xu and Arjan Thijssen from TU Delft, and Jonathan Valderrama from UTFSM for their assistance in this research. The authors also

acknowledge Rogelio Zúñiga from Asfalcura for donating the materials used in this research, and the Direction of Research from UDD for providing the funding to complete this research at TU Delft.

References

[1] Y. Huang, Pavement Analysis and Design, second ed., Pearson Prentice Hall, Upper Saddle River, NJ, 2004.
[2] EAPA, European Asphalt Association, [Online], Available: <http://www.eapa.org/asphalt.php>, (accessed: 01-Aug-2017).
[3] N. Thom, Principles of Pavement Engineering, second ed., London, 2014.
[4] Linbing Wang, Mechanics of Asphalt, first ed., McGraw-Hill, 2011.
[5] B. Picoux, A. El Ayadi, C. Petit, Dynamic response of a flexible pavement submitted by impulsive loading, Soil Dyn. Earthquake Eng. 29 (5) (2009) 845–854.
[6] Asphalt Institute, Construction of Hot Mix Asphalt Pavements, 2003.
[7] K. Yr, D.N. Little, R.L. Lytton, Fatigue and healing characterization of asphalt mixtures, J. Mater. Civ. Eng. 15 (1) (2003) 75–83.
[8] G.D. Airey, State of the art report on ageing test methods for bituminous pavement materials, Int. J. Pavement Eng. 4 (2003) 165–176.
[9] J. Norambuena-Contreras, I. Gonzalez-Torre, Influence of geosynthetic type on retarding cracking in asphalt pavements, Constr. Build. Mater. 78 (2015) 421–429.
[10] G.D. Airey, C. Young-Kyu, State of the art report on moisture sensitivity test methods for bituminous pavement materials, Int. J. Pavement Eng. 3 (4) (2002) 355–372.
[11] P. Ayar, F. Moreno-Navarro, M.C. Rubio-Gámez, The healing capability of asphalt pavements: a state of the art review, J. Cleaner Prod. 113 (2016) 28–40.
[12] Á. García, Self-healing of open cracks in asphalt mastic, Fuel 93 (2012) 264–272.
[13] J. Gallego, M.A. Del Val, V. Contreras, A. Páez, Heating asphalt mixtures with microwaves to promote self-healing, Constr. Build. Mater. 42 (2013) 1–4.
[14] Q. Liu, Á. García, E. Schlangen, M. Van De Ven, Induction healing of asphalt mastic and porous asphalt concrete, Constr. Build. Mater. 25 (9) (2011) 3746–3752.
[15] A. Garcia, E. Schlangen, M. Van De Ven, Two ways of closing cracks on asphalt concrete pavements : microcapsules and induction heating, 573–576, 2010.
[16] A. Menozzi, A. Garcia, M.N. Partl, G. Tebaldi, P. Schuetz, Induction healing of fatigue damage in asphalt test samples, Constr. Build. Mater. 74 (2015) 162–168.
[17] J. Norambuena-contreras, Single and multiple healing of porous and dense asphalt concrete, 26(4) 2015 425–433.
[18] J. Norambuena-Contreras, R. Serpell, G. Valdés Vidal, A. González, E. Schlangen, Effect of fibres addition on the physical and mechanical properties of asphalt mixtures with crack-healing purposes by microwave radiation, Constr. Build. Mater. 127 (2016) 369–382.
[19] A. García, M. Bueno, J. Norambuena-Contreras, M.N. Partl, Induction healing of dense asphalt concrete, Constr. Build. Mater. 49 (2013) 1–7.
[20] J. Norambuena-Contreras, V. Gutierrez Aguilar, I. Gonzalez-Torre, Physical and mechanical behaviour of a fibre-reinforced rubber membrane with self-healing purposes via microwave heating, Constr. Build. Mater. 94 (2015) 45–56.
[21] M.A. Franesqui, J. Yepes, C. García-González, Top-down cracking self-healing of asphalt pavements with steel filler from industrial waste applying microwaves, Constr. Build. Mater. 149 (2017) 612–620.
[22] A. Copeland, Reclaimed Asphalt Pavement in Asphalt Mixtures: State of the Practice, Rep. No. FHWA-HRT-11-021, no. FHWA, p. McLean, Virginia, 2011.
[23] S. Miliutenko, A. Björklund, A. Carlsson, Opportunities for environmentally improved asphalt recycling: the example of Sweden, J. Cleaner Prod. 43 (2013) 156–165.
[24] S. Liu, A. Shukla, T. Nandra, Technological, environmental and economic aspects of asphalt recycling for road construction, Renewable Sustainable Energy Rev. 75 (2017) 879–893.
[25] G. Thenoux, Á. González, R. Dowling, Energy consumption comparison for different asphalt pavements rehabilitation techniques used in Chile, Resour. Conserv. Recycl. 49 (4) (2007) 325–339.
[26] J. Schindelin, I. Arganda-Carreras, E. Frise, V. Kaynig, M. Longair, T. Pietzsch, S. Preibisch, C. Rueden, S. Saalfeld, B. Schmid, J.-Y. Tinevez, D.J. White, V. Hartenstein, K. Eliceiri, P. Tomancak, A. Cardona, Fiji: an open-source platform for biological-image analysis, Nat. Methods 9 (7) (Jul. 2012) 676–682.
[27] CSN, Bituminous mixtures. Test methods for hot mix asphalt. Stiffness, 2012.
[28] O. GmbH, Optris PI Connect, 2014.
[29] The Mathworks, Matlab, Natick, 2012.
[30] A. García, J. Norambuena-contreras, M. N. Partl, P. Schuetz, Uniformity and mechanical properties of dense asphalt concrete with steel wool fibers, 43, 2013, 107–117.
[31] P. Li, Z. Ding, Analysis of viscous flow properties of asphalt in aging process, Constr. Build. Mater. 124 (2016) 631–638.
[32] J. Norambuena-Contreras, A. Garcia, Self-healing of asphalt mixture by microwave and induction heating, Mater. Des. 106 (2016) 404–414.
[33] Y. Sun, S. Wu, Q. Liu, W. Zeng, Z. Chen, Q. Ye, P. Pan, Self-healing performance of asphalt mixtures through heating fibers or aggregate, Constr. Build. Mater. 150 (2017) 673–680.
[34] R.K. Amankwah, G. Ofori-Sarpong, Microwave heating of gold ores for enhanced grindability and cyanide amenability, Miner. Eng. 24 (6) (2011) 541–544.
[35] E.R. Bobicki, Q. Liu, Z. Xu, Microwave heating of ultramafic nickel ores and mineralogical effects, Miner. Eng. 58 (2014) 22–25.
[36] Volume graphics, VG Studio Max 3.0.